Loss of both phospholipid and triglyceride transfer activities of microsomal triglyceride transfer protein in abetalipoproteinemia

Irani Khatun,*,†,§ Meghan T. Walsh,*,†,§ and M. Mahmood Hussain[1],†,§

Molecular and Cellular Biology Program,* School of Graduate Studies, Department of Cell Biology,† and Department of Pediatrics,§ SUNY Downstate Medical Center, Brooklyn, NY

Abstract Mutations in microsomal triglyceride transfer protein (MTP) cause abetalipoproteinemia (ABL), characterized by the absence of plasma apoB-containing lipoproteins. In this study, we characterized the effects of various MTP missense mutations found in ABL patients with respect to their expression, subcellular location, and interaction with protein disulfide isomerase (PDI). In addition, we characterized functional properties by analyzing phospholipid and triglyceride transfer activities and studied their ability to support apoB secretion. All the mutants colocalized with calnexin and interacted with PDI. We found that R540H and N780Y, known to be deficient in triglyceride transfer activity, also lacked phospholipid transfer activity. Novel mutants S590I and G746E did not transfer triglycerides and phospholipids and did not assist in apoB secretion. In contrast, D384A displayed both triglyceride and phospholipid transfer activities and supported apoB secretion. These studies point out that ABL is associated with the absence of both triglyceride and phospholipid transfer activities in MTP.— Khatun, I., M. T. Walsh, and M. M. Hussain. **Loss of both phospholipid and triglyceride transfer activities of microsomal triglyceride transfer protein in abetalipoproteinemia. *J. Lipid Res.* 2013.** 54: **1541–1549.**

Supplementary key words apolipoprotein B • lipoproteins • mutations

Microsomal triglyceride transfer protein (MTP) is a heterodimer of a large ~97 kDa M subunit and a ~55 kDa protein disulfide isomerase (PDI) P subunit held together by noncovalent interactions in 1:1 stoichiometry (1–4). PDI helps to maintain solubility and retention of MTP in the endoplasmic reticulum (ER) (1, 2). The M-subunit of MTP is a single peptide of 894 amino acids. Based on its homology with lipovitellin, an ancient transport and storage lipoprotein found in egg-laying vertebrates, MTP has been predicted to contain three major structural domains: N- terminal β-barrel (amino acids 22–297), central α-helical region (amino acids 298–603), and C-terminal domain (amino acids 604–894) (5–8). Based on mutagenesis followed by functional studies, it has been suggested that the N-terminal domain binds apoB (7), the central α-helical region interacts with both PDI and apoB (9), and the C-terminal domain is involved in lipid binding and transfer (7). Bakillah et al. (10) identified small-molecule inhibitors that differentially inhibit MTP's lipid transfer and apoB-binding activities, providing evidence for different functional domains. Further, it has been suggested that different domains of MTP carry out different functions (8, 11).

MTP facilitates transfer of lipids to nascent apoB while it is being cotranslationally translocated across the ER membrane, thereby aiding in the assembly of primordial lipoprotein particles and preventing presecretory proteasomal degradation of apoB (12). Kinetic studies predict that MTP has two lipid binding sites (13, 14); the fast site is implicated in triglyceride and phospholipid transfer, whereas the slow site in phospholipid transfer only. Evolutionary studies have suggested that MTP evolved as a phospholipid transfer protein and acquired triglyceride transfer during a transition from invertebrates to vertebrates (15). Further, it was shown that phospholipid transfer activity of MTP is sufficient to support secretion of apoB-containing lipoproteins in vitro and in vivo (16, 17).

Abetalipoproteinemia (ABL, OMIM#200100) is a rare autosomal recessive disorder due to mutations in the *MTTP* gene. Plasma triglycerides (<0.23 mmol/l, 20 mg/dl) and cholesterol (<1.16 mmol/l, 45 mg/dl) are typically low; in addition, LDL and apoB are undetectable. Acanthocytosis of red blood cells is a distinguishing feature on blood smears (18). The severity of symptoms varies, and their

This work was supported by National Institutes of Health Grants DK-46900 and HL-095924 (to M.M.H.) and American Heart Association Predoctoral Fellowship 3230023 (to I.K.).

Manuscript received 27 August 2012 and in revised form 7 March 2013.

Published, JLR Papers in Press, March 8, 2013
DOI 10.1194/jlr.M031658

Abbreviations: ABL, abetalipoproteinemia; ER, endoplasmic reticulum; hMTP, human MTP; MTP, microsomal triglyceride transfer protein; PDI, protein disulfide isomerase; PL, phospholipid; TG, triglyceride.

[1] To whom correspondence should be addressed.
e-mail: Mahmood.Hussain@downstate.edu

Copyright © 2013 by the American Society for Biochemistry and Molecular Biology, Inc.

This article is available online at http://www.jlr.org

subsequent downstream complications depend on early diagnosis and treatment. During the first and second decade, the first symptoms to be noticed are fat malabsorption, steatorrhea, and failure to thrive. The other ramifications of the disease are fat-soluble vitamin deficiency, specifically vitamin E (19) and vitamin A, as apoB-containing lipoproteins distribute these vitamins to the peripheral tissues. The most prominent and debilitating clinical manifestations of ABL are neurological disorders caused by the deficiency of vitamin E and progressive degeneration of the central nervous system, leading to death.

The majority of the mutations reported following sequence analysis of the MTP gene or cDNA in ABL subjects are frameshift, nonsense, and splice site mutations that are predicted to encode truncated forms of MTP completely devoid of function (20–28). However, a few missense mutations, R540H (23, 25), S590I (25, 29), N780Y (7, 26), D384A (23, 30), and G746E (25) have been described. Characterization of some of these mutants has provided significant information about the structure-function of MTP. Ricci et al. reported a nonsense mutation, G865× that caused loss of 30 amino acids at the C-terminal β-sheet of the 97 kDa MTP subunit (31). The translated protein lost the ability to interact with PDI and was unable to transfer lipids, indicating that C-terminal β-sheet may play a role in the formation of the active heterodimer. N780Y, located in the C-terminal end, has been shown to interact with PDI but lacks triglyceride transfer activity (7, 26). It has been suggested to interact with membranes and extract lipids for transfer (7). It does not support secretion of apoB41 but does support secretion of vitellogenin (32). R540H neither transfers triglycerides nor supports apoB secretion (23). It has been suggested to form an internal salt bridge to keep the central α-helical domain in proper conformation for PDI binding (6). However, nothing is known about the ability of these two missense mutants to transfer phospholipids. ABL subjects homozygous for S590I have been reported (25), but the biochemical reason for the disease phenotype has not been explained. In contrast, D384A and G746E have been reported as compound heterozygotes with other mutations, and therefore, it is not known whether these mutations affect MTP activity and contribute to the ABL phenotype (23, 25, 30). In this study, we explored the effects of these missense mutations on various aspects of cellular, molecular, and biochemical properties of MTP.

MATERIALS AND METHODS

Materials

Four to 15% ready Tris-HCl gels and precision-plus protein ladder were obtained from Bio-Rad Laboratories. β-mercaptoethanol and restore western blot stripping buffer were purchased from Invitrogen and Thermo Scientific, respectively. Calcium chloride, ethylene diamine tetraacetic acid, Hepes, kanamycin, magnesium chloride, molecular weight markers, oleic acid, Tween-20, and Triton X-100 were bought from Sigma. Glycerol, heparinized micro-hematocrit capillary tubes, sodium dodecyl sulfate, and sucrose were obtained from Fisher Chemicals. Fugene and lipofectamine were obtained from Roche and Invitrogen, respectively. Antibodies M2 FLAG, anti-human apoB, anti-human PDI, anti-human GAPDH, and Alexa Fluor 488 and 594 were purchased from Molecular Probes.

Cloning and generation of recombinant retroviruses

Single amino acid mutations for each missense mutation were introduced in FLAG-tagged human MTP (hMTP-FLAG) (33) sequence using site-directed mutagenesis (Stratagene). Mutagenesis was confirmed by sequencing. Later these mutations were cloned into a pMFG retroviral vector. Human kidney-derived cell line 293GPG was used for retroviral packaging. pMFG retroviral vectors carrying normal and mutant MTP were transiently transfected using lipopfectamine 2000 (Invitrogen) according to the manufacturer's instructions. Viruses were harvested 48–72 h following transfection in tet-off media to initiate viral production. The viral supernatants were collected and amplified on large scale and subsequently used to generate stable cell lines.

Generation of stable cell lines expressing MTP mutations

Monkey kidney COS7 cells (2×10^5), which do not express MTP and apoB, were seeded in tissue culture plates. These cells were transduced with recombinant retroviruses and were grown to confluence. This infection step was repeated three times; cells were stored in liquid nitrogen. As all the proteins generated were FLAG tagged, FLAG expression was quantified by western blot analysis to compare protein levels.

Cell culture and apoB secretion studies

COS7 cell lines stably expressing different mutants were grown in Dulbecco's modified Eagle's medium (CellGrow) containing 10% fetal bovine serum supplemented with L-glutamine and antibiotics. ApoB expression vectors were transfected into these cells using FuGENE 6 (Roche Applied Sciences) according to the instructions provided by the manufacturer. The cells were detached from the plate after 8–10 h using trypsin and were plated in 6-well plates (400,000 cells/well). During the final 16 h of 48 h post transfection, media were replaced with either 1 ml of DMEM with 1.5% BSA or DMEM containing 0.4 mM oleic acid complexed with 1.5% BSA and 1 mM glycerol. Media and cells were collected in tubes containing protease inhibitors (Sigma-Aldrich). Media were centrifuged and supernatants were used to measure apoB by ELISA (34, 35). Cells were used to measure intracellular apoB. For this purpose, cells were scraped in cold PBS, and a small sample was taken for total protein measurement. After centrifugation for 5 min at 100 *g*, pellets were lysed in cell extract buffer (100 mM Tris, pH 7.4, 150 mM NaCl, 1 mM EGTA, 1 mM EDTA,1% Triton X-100, 0.5% sodium deoxycholate) and rotated for 1 h at 4°C. The cell extract was centrifuged at 16,000 *g*, and the supernatant was used to measure apoB by ELISA (34). Intracellular apoB was normalized to total cell protein.

Immunofluoroscence

Stable cell lines were grown on coverslips in 12-well cell culture plates, fixed, blocked, and probed with primary and secondary antibodies as described earlier (16). Cells were incubated with 0.05% Tween 20 in 10 mM sodium citrate buffer (pH 6.0) at 37°C for 15–20 min. PBS containing 1 mM $MgCl_2$, 0.5 mM $CaCl_2$, 3% BSA, and 1% horse serum was used as blocking reagent. Primary and secondary antibody dilutions were made in the same buffer. The cells were incubated for 1 h with 1:100 dilution of mouse anti-FLAG M2 (Sigma) and rabbit anti-PDI (AbCam) or rabbit anti-calnexin (Santa Cruz Biotechnology) for 1 h with 0.1% Triton-X100 to increase the permeability. Alexa Fluor 488-conjugated goat anti-rabbit IgG1 (green fluorescence) and Alexa

Fluor 594-conjugated goat anti-mouse IgG1 (red fluorescence) (Molecular Probes) were incubated for 1 h following primary antibody treatment. The coverslips were mounted in anti-fade (Vectashield) to prevent fluorescent bleaching and analyzed with a laser-scanning microscope (Model LSM 510, Carl Zeiss). Images were imported and analyzed with Photoshop 6.0 before exporting to Illustrator CS2 (Adobe).

Lipid transfer assays

Lipid transfer activities of MTP in COS7 cells stably expressing different mutants were determined by triglyceride and phospholipid transfer assays as described earlier (36, 37). Cells were extensively washed in ice-cold PBS and homogenized in 1 ml of ice-cold homogenizing buffer (Tris-HCl, pH 7.6, 1 mM EGTA, and 1 mM MgCl2) containing protease inhibitor cocktail (Sigma) using a Dounce homogenizer. This low-salt buffer is known to disrupt microsomes and release its contents (36). Homogenates were centrifuged in a SW55 Ti rotor at 50,000 rpm for 1 h at 10°C. To purify proteins, homogenates were incubated with M2 agarose beads (Sigma) and eluted three times with FLAG fusion peptide (150 ng/μl) (Sigma). Supernatants were used for MTP lipid transfer assays in triplicates as described elsewhere (36, 37). In brief, homogenates were added to a mixture of donor vesicles containing NBD-triglycerides and acceptor vesicles. After 30 min, increases in fluorescence due to transfer were recorded. Total fluorescence was measured by disrupting vesicles with isopropanol. Fluorescence values containing no MTP as blank were subtracted from samples containing MTP proteins and divided by the total fluorescence of vesicles to determine percentage of lipid transfer. Similarly, phospholipid transfer assays were performed (37). Again, purified proteins were added to a mixture of donor vesicles containing NBD-phosphatidylethanolamine and acceptor vesicles. Increase in fluorescence was measured, and percentage lipid transfer was determined by subtracting fluorescence values containing no MTP from samples containing MTP divided by total fluorescence of vesicles obtained after their disruption with isopropanol.

Immunoprecipitation and western blot analysis

For coimmunoprecipitation of MTP and PDI, COS7 cells stably expressing different mutants were grown, washed with PBS, scraped, and collected. Cells were homogenized as described above, and protein content in homogenates was determined by Bradford assay (Thermo Scientific). Equal amounts of total proteins (adjusted with 150 mM NaCl, pH 7.4, if necessary) from different cell lines were incubated with mouse-anti-FLAG antibody according to manufacturer's recommendations at 4°C overnight. Protein A/G agarose beads from Santa Cruz Biotechnology were added the next morning and further incubated for 2 h. Beads were pelleted, washed, and resuspended in 1× SDS-PAGE laemmeli buffer. Beads were spun down after boiling, and the supernatant containing the immunoprecipitated proteins were applied to 4-20% precast SDS-PAGE gel (Bio-Rad), subjected to electrophoresis, transferred onto nitrocellulose membrane, and probed for protein expression, FLAG, and PDI.

mRNA quantifications

Total RNA from cells was isolated using TriZol (Invitrogen). The first-strand cDNA was synthesized using Omniscript RT (Qiagen) kit. Each reaction of quantitative RT-PCR was carried out in a volume of 20 μl, consisting of 9 μl cDNA sample (1:50 dilution of the first strand cDNA sample) and 11 μl of PCR master mix solution containing 1× PCR reaction buffer (qPCR Core Kit for SYBR Green I, Eurogentec). The PCR was carried out by incubating the reaction mixture first for 10 min at 95°C, followed by 40 cycles of 15 s incubations at 95°C and 1 min at 60°C in the ABI 7000 SDS PCR machine. Data were analyzed using $\Delta\Delta C_T$ method according to manufacturer's instruction and are presented as arbitrary units. Data were normalized to 18S rRNA.

Statistical analyses

One-way ANOVA was performed to compare differences between groups. Comparisons were made between COS7 cells expressing hMTP and all other mutations, and significant differences are depicted by asterisks. Each analysis was performed in triplicate, and mean values were used as one value. Data represent the average of triplicate values and their SEM. Data are representative of two to three independent experiments.

RESULTS

Structural illustration and location of missense mutations in MTP protein

A diagram of the secondary structure of MTP based on PSIPRED secondary structure prediction (38) overlaid on the primary sequence shows N- and C-terminal β-sheets and a central α-helical domain (**Fig. 1A**). Various ABL missense mutations have been identified to highlight their location in different regions of the protein (Fig. 1A). A schematic illustration of the secondary structure of MTP with respect to different predicted structural domains is shown in Fig. 1B, along with location of the mutations. A predicted tertiary structure build on lipovitellin (5, 39) illustrates different structural domains and the location of different mutants (Fig. 1C, D). These analyses showed that mutations D384A, R540H, and S590I are located in the central α-helical domain, whereas G746E and N780Y are in the C-terminal β^A sheet domain.

Expression of MTP mutants in stably transfected cells

To study the importance of various amino acid residues, site-directed mutagenesis was employed to create individual missense mutations into the coding sequence of wild-type human MTP 97 kDa subunit. These mutants were sequenced, cloned in the retrovirus expression vector pMFG-hMTP-FLAG, and stably expressed in COS7 cells that lack endogenous expression of apoB and MTP. Cells stably expressing pMFG-hMTP-FLAG were used as positive controls.

To determine whether single amino acid substitutions affect expression, we performed immunofluorescence using anti-FLAG antibodies. All mutant proteins could be detected in different cell lines (**Fig. 2**). To determine the subcellular location of these mutant proteins, cells were also stained for calnexin, an ER marker (Fig. 2). Merging of the calnexin- and FLAG-stained images showed overlap (yellow), suggesting their juxtaposition (Fig. 2). This expression pattern is consistent with those of human and *Drosophila* MTP reported earlier (16, 17). These data demonstrate that MTP mutants are expressed in these cells and localize similarly to hMTP in cells.

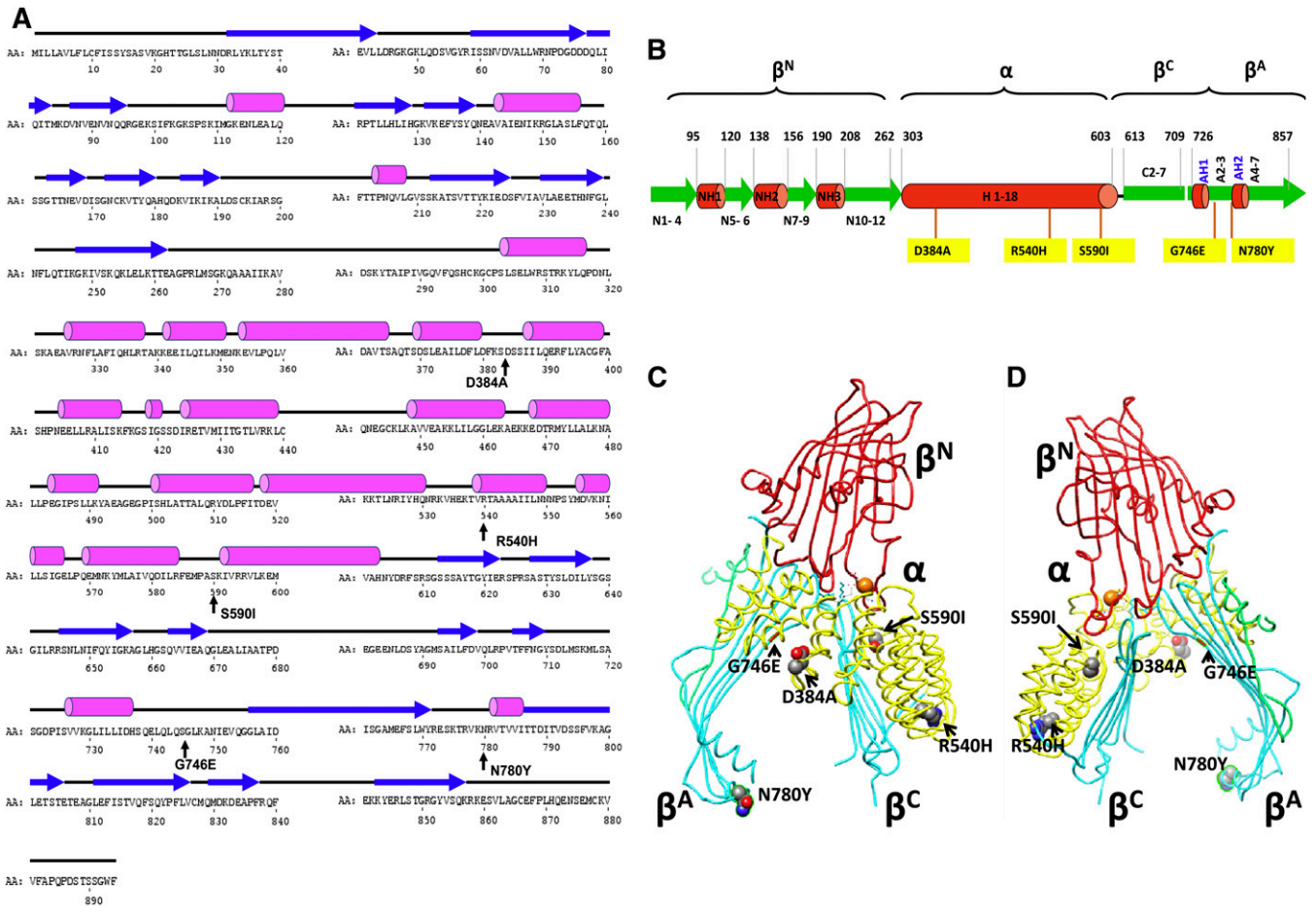

Fig. 1. Amino acid sequence as well as predicted secondary and tertiary structural domains of MTP. (A) Predicted secondary structural domains (top row) of MTP were drawn manually on top of the amino acid residues (second row) based on PSIPRED (38) and homology modeling published earlier (8). The bold blue arrows represent β-sheet, whereas pink barrels represent α-helices. The third row shows number of amino acid residues. The missense mutations and their locations have been identified with black arrows. (B) A schematic line diagram of the 97 kDa MTP subunit showing all the putative structural domains. The N-terminal β-sheet (β^N, amino acids 22–297) contains three helices (NH1–NH3) and 12 β-sheets (N1–N12). The central α-helical domain (α, 298–603) contains 18 helices (H1–18). The C-terminal β-sheet (604–894) contains two β-sheet domains: β^C or C-sheet (C2–7) and β^A or A-sheet (A2–7). The A-sheet also contains two short highly conserved α-helices, AH1 and AH2. The missense mutations cloned and characterized in this study have been identified. (C) Tertiary structure of MTP was built using Chimera based on lipovitellin structure. Ribbon diagram of different domains have been differentially color coded: β^N, red; α-helix, yellow; β^C and β^A, cyan. The ABL mutants are shown in the structure. Side chains of residues depicting atoms/bonds are represented as spheres showing van der Waals radii. The colors denote nitrogen in blue, carbon in gray, and oxygen in red. (D) The posterior view of the MTP protein is shown for better representation of residues S590 and R540.

Heterodimerization of MTP mutants with PDI

MTP and PDI subunits form heterodimers with a stoichiometry of 1:1 (2, 3). This heterodimer formation is required to facilitate lipid transfer activity. Therefore, we performed immunofluorescence and coimmunoprecipitation analysis to study interactions between MTP and PDI subunits in COS7 cells stably expressing different MTP mutants (**Fig. 3**). Staining was seen for both MTP-FLAG and PDI in cells expressing hMTP and all other mutants. Overlap of MTP-FLAG and PDI was evident as yellow in merged images in most cell lines. In R540H-expressing cells, there was less yellow color, indicative of possibly sparse colocalization of these subunits (Fig. 3). Alternatively, this could be due to low intensity of the FLAG signal. These data indicate that, except for R540H, all mutant proteins are in close proximity of PDI in these cells.

We next determined whether MTP mutants coimmunoprecipitate with PDI. FLAG proteins were immunoprecipitated using anti-FLAG M2 antibodies, and immunoprecipitated proteins were western blotted to detect MTP. Membranes were stripped and reprobed with anti-PDI antibodies (**Fig. 4**). No FLAG protein or PDI was detected in wild-type control cells, indicating absence of proteins recognized by anti-FLAG antibodies in these cells. Immunoprecipitates obtained from COS7 cells expressing D384A, S590I, G746E, and N780Y contained both FLAG and PDI (Fig. 4A); however, lower amounts of PDI were precipitated with R540H-FLAG consistent with Mann et al. (6). PDI/MTP ratios after the densitometric quantifications of bands are shown in Fig. 4B. In most cases, this ratio ranged between 0.7 and 1.0, but it was lower for R540H. These studies show that that all mutants, except for R540H, interact strongly

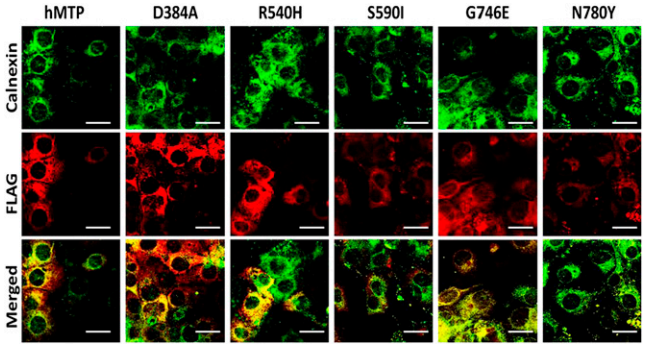

Fig. 2. Expression and subcellular localization of hMTP mutants. COS7 cells stably expressing hMTP or different mutants were fixed, permeabilized, blocked, and probed with primary antibodies for FLAG and Calnexin. Subsequently, they were probed with Alexa Fluor 488 (Calnexin, green) and Alexa Fluor 594 (FLAG, red) conjugated secondary antibodies. Immunofluoroscence was detected using a Carl Zeiss confocal microscope. Images were merged to detect colocalization of the proteins. Duplicate samples were processed and several fields were scanned. Representative images are shown. The bar represents 20 μm.

with endogenous PDI. The reasons for low association of PDI with R540H are not known. It is likely that interactions between R540H and PDI are weaker than those of other MTP mutants.

Effect of missense mutations on distinct lipid transfer activities of MTP

First, we studied the expression of different mutants in duplicate cell cultures by measuring MTP mRNA levels (**Fig. 5A**). All cell lines, except for D384A that showed higher mRNA levels, had similar levels of transcripts. To assay different lipid transfer activities, proteins were purified using anti-FLAG antibodies. Purification was necessary, as we could not reliably measure phospholipid transfer activities in either cell homogenates or microsomal lumenal contents. Western blot analysis showed that, except for the lower levels of G746E, we were able to purify different mutants and hMTP to similar extents (Fig. 5B). Next, we examined triglyceride transfer activity in these purified proteins (Fig. 5C). Significant triglyceride transfer activity was measurable in purified hMTP (Fig. 5C). D384A exhibited significant triglyceride transfer activity, but it was lower than hMTP. In contrast, no triglyceride transfer activity was measurable in R540H, S590I, G746E, or N780Y mutants. Besides triglyceride transfer, MTP also transfers phospholipids. Similar levels of phospholipid transfer activities were exhibited by hMTP and D384A. But no phospholipid transfer activity was measurable in R540H, S590I, G746E, or N780Y mutants (Fig. 5D). These studies show that R540H, S590I, G746E, and N780Y are deficient in both triglyceride and phospholipid transfer activities.

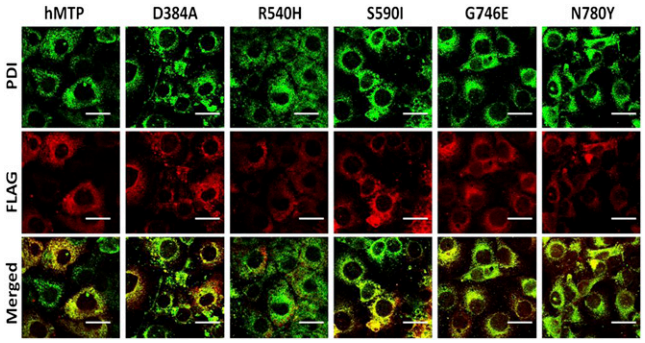

Fig. 3. MTP and PDI interaction. COS7 cells stably expressing hMTP or different mutants were reacted with anti-PDI and anti-FLAG antibodies. They were then probed with Alexa Fluor 488 (PDI) and Alexa Fluor 594 (FLAG). Immunofluorescence was detected using a Carl Zeiss confocal microscope. Images were merged to detect colocalization of the proteins. Duplicate samples were processed and several fields were scanned. Representative images are shown. The bar represents 20 μm.

Ability of different missense mutations to support apoB lipoprotein assembly and secretion

The major function of MTP is to support apoB lipoprotein assembly and secretion. To study apoB secretion, various cell lines stably expressing hMTP and different mutants were transiently transfected with apoB48-expressing plasmid. Different experiments were performed to measure intracellular apoB mRNA and protein levels. **Fig. 6A** shows the mRNA levels of apoB in two different dishes of various cell lines (Fig. 6A). All dishes had similar apoB mRNA levels, except for one dish expressing N780Y. These studies indicated significant expression of apoB. We also measured MTP expression in different wells. Fig. 6B shows the expression of different MTPs at the end of the experiment in two different wells. To study apoB secretion, we quantified media apoB. ApoB was detectable in the media of cells stably expressing hMTP and D384A, but it was not detectable in cells expressing R540H, S590I, G746E, or N780Y (Fig. 6C). To eliminate the possibility that low availability of lipids affected apoB secretion, cells were supplemented with oleic acid complexed to BSA. ApoB secretion was enhanced by ~40% in cells expressing hMTP or D384A (Fig. 6D) when compared with cells that were not supplemented with oleic acid (Fig. 6C). However, apoB was still not detectable in the media of cells expressing R540H, S590I, G746E, or N780Y mutants. Consideration was given to the possibility that lack of apoB expression might be secondary to no cellular apoB protein. Cells were transfected with apoB48-expressing plasmids, and intracellular apoB levels were quantified by ELISA (Fig. 6E). There were similar amounts of intracellular apoB in all cell lines, indicating significant and equal expression. Thus, hMTP and D384 support apoB48 secretion, but other mutants do not.

DISCUSSION

Although it is established that MTP is indispensable for apoB lipoprotein assembly and secretion, gathering information about the structure and function of MTP has been hard due to difficulties in obtaining a three-dimensional X-ray crytallographic structure. Identification of missense mutations in the M subunit as the prime cause of ABL provided a possible new approach to explore structure-function

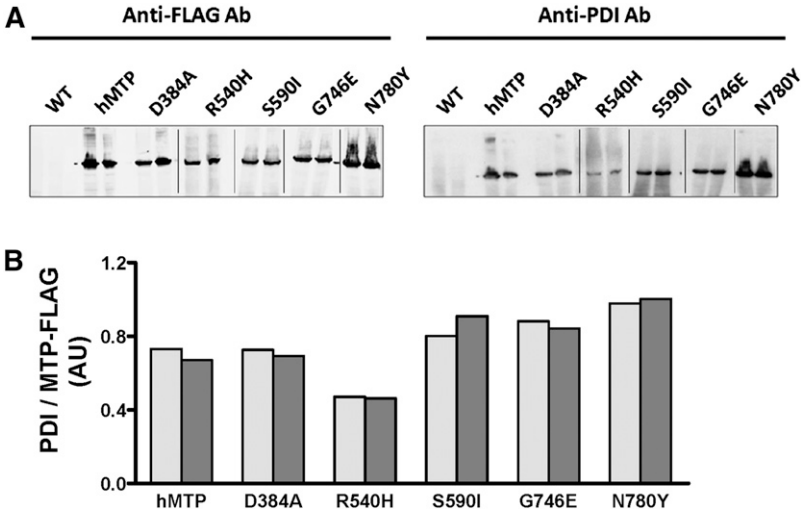

Fig. 4. Coimmunoprecipitation studies showing MTP and PDI interactions. Wild-type COS7 cells and cell lines stably expressing hMTP or different mutants were seeded and grown to confluence. (A) Homogenates from two different dishes were prepared and used to immunoprecipitate chimeric proteins using FLAG antibody. Immunoprecipitated proteins were separated on 4–20% SDS-PAGE gels and transferred to nitrocellulose membranes. Western blot analyses were performed for FLAG-tagged MTP proteins using M2 anti-FLAG antibody (left panel). Membranes were stripped, and western blot analyses were performed for PDI proteins using rabbit anti-human PDI antibody (right panel). (B) Relative ratios of PDI and MTP (FLAG) in duplicate for each mutant were quantified from gels shown in (A).

relationships. We analyzed the effects of different reported ABL missense mutations on MTP function. Our studies confirm previous observations that R540H mutant neither transfers triglyceride nor supports apoB secretion, whereas D384A does both (23). Similarly, we also observed that N780Y interacts with PDI but does not transfer triglyceride as has been shown before (7, 26). Further, our studies show that this missense mutation is incapable of supporting apoB48 secretion as has been reported for apoB41 (32). We extend these studies to show that R540H and N780Y mutants also lack phospholipid transfer activity. Additionally, we report for the first time that S590I and G746E do not support apoB secretion. To identify mechanisms for their inability to support apoB secretion, we examined ER localization, interaction with PDI, and both triglyceride and phospholipid lipid transfer activities. These mutants interacted with PDI, but were unable to transfer lipids. Thus, a proximal reason for ABL due to R540H, S590I, G746E, or N780Y missense mutations might be the absence of both triglyceride and phospholipid transfer activities.

S590I missense mutation was described in a 52-year-old subject with a lifelong history of fat malabsorption (29) and in a 24-year-old subject (25), suggesting that this mutation might result in a milder ABL phenotype. Despite the milder clinical phenotype, these patients lacked plasma apoB-containing lipoproteins and showed acanthocytosis. It had been suggested that this mutation might not have a major impact on the synthesis and function of MTP (29). Our in vitro studies, however, showed that MTP with this mutation has no lipid transfer activity and is unable to support assembly and secretion of apoB48-containing lipoproteins. Thus, this mutation has severe biochemical defects. These data explain the absence of apoB-containing lipoproteins in these patients, but they do not provide any explanation regarding milder clinical phenotype, especially with regards to the absence of neuropathy usually associated with vitamin E deficiency. It is possible that these subjects might have upregulated an alternate mechanism of absorbing vitamin E independent of apoB lipoproteins, such as those involving transport via HDL, despite having low levels (40, 41).

S590 is located in the loop between helices 17 (amino acids 569–584) and 18 (amino acids 591–603) of the central α-helical region (**Fig. 7A**). It has been suggested (6) that residues I592, Y554, M555, and K558 (Fig. 7B) are involved in PDI binding, as combined mutagenesis of Y554, M554, and I592 to alanine severely curtails PDI binding and triglyceride transfer activity. However, individual K591A, I592A, R594A, R595A, K598A, and E599A (Fig. 7C) substitutions had very small effects on MTP activity (6). Thus, it was surprising to see that S590I resulted in complete loss of MTP activity. It has been previously pointed out (6) that S590 could be part of a hydrophobic patch at the edge of the helical domain, along with F585, M587, and A589 (Fig. 7B). S590I would increase hydrophobicity of the pocket. We noticed that S590 could also potentially form a hydrogen bond with M587 besides participating in the formation of a hydrophobic pocket between helices 17 and 18 (Fig. 7B, C). Further mutagenesis experiments are needed to resolve whether S590 is crucial because it contributes to an optimum hydrophobic pocket or because its interaction with M587 is important for MTP activity.

G746E was reported as a compound heterozygote in an ABL subject (25); the other mutation found in this subject was a nonsense mutation resulting in the synthesis of a truncated protein. Therefore, it was not clear whether G746E contributes to the ABL phenotype. Our studies show that G746E missense mutation is accompanied with loss of triglyceride and phospholipid transfer activities in MTP and does not support apoB secretion. Thus, G746E alone could cause ABL. G746E is located in the deep pocket of MTP lipid transfer domain (Fig. 7D). We predict that introduction of a charged residue in this hydrophobic pocket might hinder neutral lipid acquisition for transfer. Thus, conversion of glycine to glutamic acid might create a hydrophilic environment untenable for the transfer of hydrophobic lipids.

Individuals homozygous for D384A have not been identified; instead, this mutation has been presented as compound heterozygote with R540H (23). Therefore, physiologic effects of this mutation are unknown. We found that D384A has no significant impact on PDI binding, lipid transfer

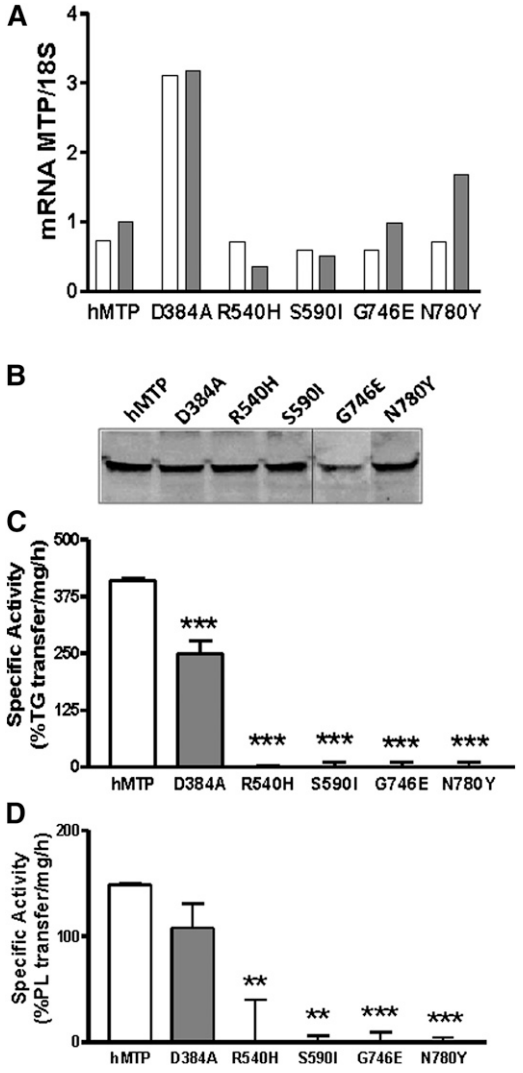

Fig. 5. Lipid transfer activities of different MTP mutants. COS7 cell lines stably expressing hMTP or different mutants were seeded and grown to confluence. (A) MTP mRNA levels were measured in two different dishes of individual cell lines by qRT-PCR and normalized to 18S rRNA. (B) Different indicated proteins were purified using anti-FLAG antibodies from various indicated cell lines. Western blot analyses were performed to ascertain purification. Equal amounts of proteins were used to determine (C) triglyceride and (D) phospholipid transfer activities. Data are representative of two independent experiments. Mean ± SEM, n = 3. One-way ANOVA was performed to compare differences between groups. $^{**}P < 0.01$, $^{***}P < 0.001$.

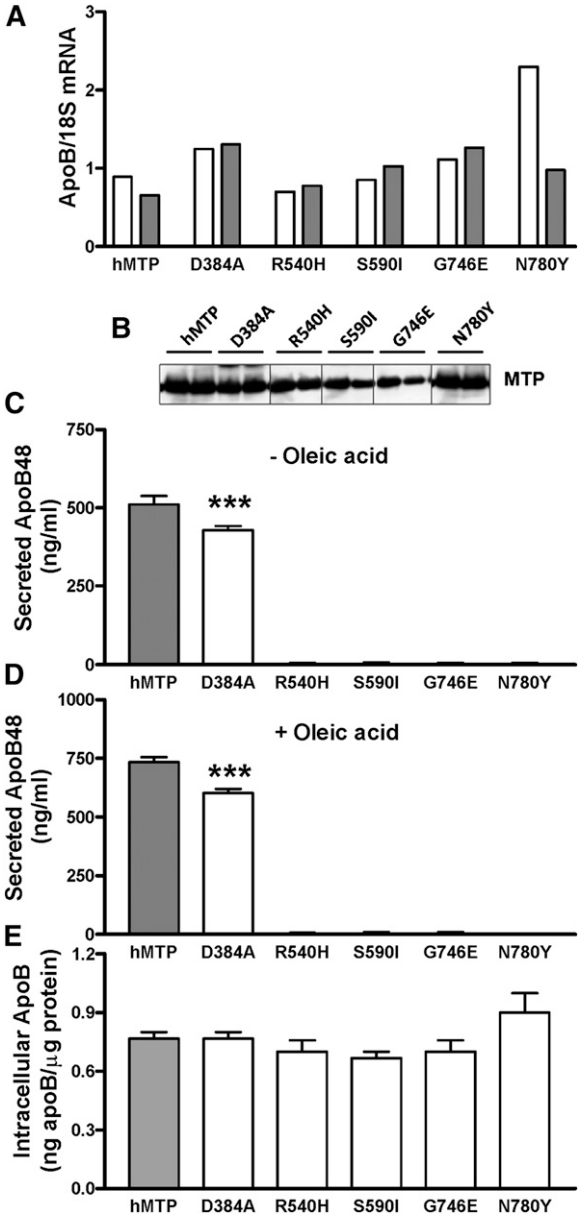

Fig. 6. ApoB secretion supported by MTP mutants. ApoB expression plasmids were transiently transfected in COS7 cells expressing hMTP or different indicated MTP mutants. (A) ApoB mRNA levels were quantified from two different wells of individual cell lines transfected with a human apoB48 expression plasmid. (B) Western blot analyses of the purified MTP proteins are shown for the respective groups to depict FLAG expression. (C) Media from different cell lines was used to quantify apoB48 by ELISA. (D) ApoB secretion supported by MTP mutants during higher lipid availability was studied by supplementing cells with 0.4 mM oleic acid complexed with 1.5% BSA and 1 mM glycerol for the last 16 h of incubation. Media apoB was quantified by ELISA and concentrations were calculated from known standards. (E) Cells were used to measure intracellular apoB levels by ELISA. Data represent mean ± SEM, n = 3. One-way ANOVA was performed to compare differences between groups. $^{***}P < 0.001$.

activities, or apoB secretion, consistent with other studies (23). Hence, D384A is a polymorphism located in a highly conserved region of MTP, and individuals homozygous for this mutation may not have significant phenotype. This is surprising, as a mutation from D to A leading to loss of a negative charge is expected to cause significant structural changes. However, D384 is located between helices H5 (369–380) and H6 (386–398) of the central α-helical domain and is predicted to be surface accessible by Michel Sanner's molecular surface (MSMS) analysis (42). Thus, a reason for no effect on MTP activity could be that due to its location on the surface of the molecule, it is not critical for lipid transfer.

R540 is within the helix H15 (537-550) of the central α-helical domain and is not surface accessible. It has been suggested to form an internal salt bridge with E570 and N531 between helices 13 and 14 and the loop before the

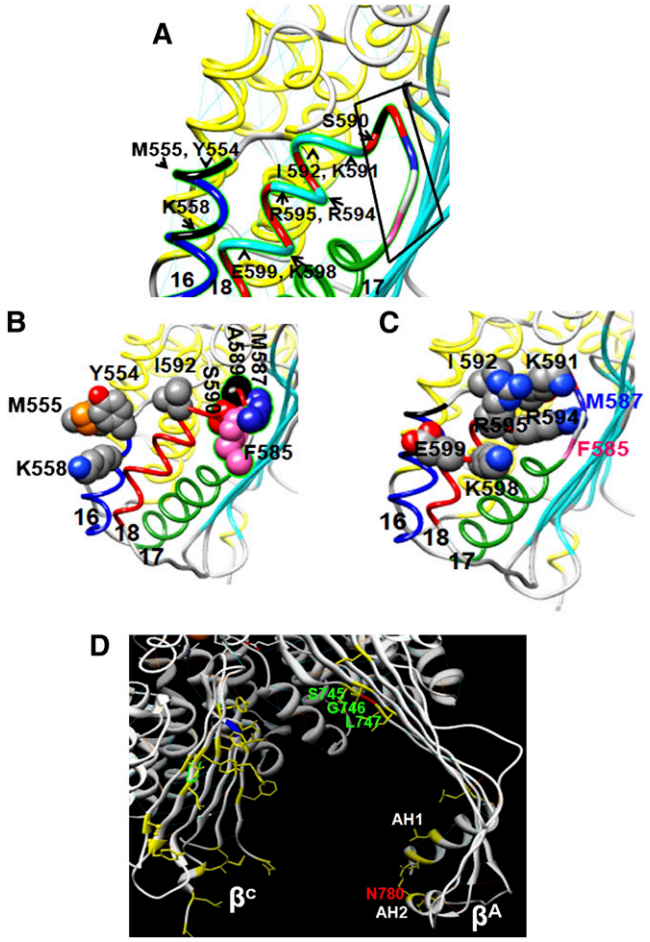

Fig. 7. Molecular model showing expanded view of S590 and G746 in the central α-helices and adjacent β^C-sheets. (A) Helices 16, 17, and 18 are highlighted as blue, green, and red ribbons, respectively. The rectangle shows the hydrophobic pocket in the loop expanded in (B). Residues Y554, M555, and K558 on helix 16 and K591, I592, R594, R595, K598, and E599 on helix 18 are highlighted in black and cyan, respectively. (B) S590 hydrophobic pocket along with residues A589 on helix 18 and F585 and M587 in the loop is shown. Also shown are side-chain atoms of residues Y554, M555, K558 (helix 16), and I592 (helix 18). Van der Waals radii for carbon, oxygen, nitrogen, and phosphorus are in gray, red, blue, and orange, respectively. (C) Detailed side-chain residues of K591, I592, R594, R595, K598, and E599 are shown with respect to the predicted hydrophobic pocket of S590. Van der Waals radii for carbon, oxygen, and nitrogen are shown in gray, red, and blue, respectively. (D) Ribbon diagram of hydrophobic lipid binding cavity of MTP flanked with C-terminal β^C-sheet and β^A-sheet is shown. Side chains of hydrophobic residues (yellow) in β^C-sheet and β^A-sheet are exposed in the cavity that could potentially interact with neutral lipids influencing lipid-binding capacity. G746 (red) in β^A-sheet flanked with hydrophobic residues S745 and L747 are also shown. AH1 and AH2 helices (yellow ribbons) in β^A-sheet are shown with hydrophobic residues with side chains exposed. Further, N780 is highlighted in red.

helix 16 (6). The R540H mutation has been shown to reduce the association of the M subunit with the PDI subunit (6). Further, it has been shown to lack triglyceride transfer activity and is unable to support apoB secretion (6, 23). We also observed that R540H interacts poorly with PDI, is unable to transfer triglycerides and phospholipids, and is incapable of assisting apoB secretion. These studies indicate that disruption of the internal salt bridge has a significant effect on MTP structure, resulting in the loss of both the lipid transfer activities.

The C-terminal β-sheet of MTP has been suggested to be crucial for its lipid transfer activity. Within this C-sheet, two α-helices, AH1 (residues 725–736) and AH2 (residues 781–786), have been proposed to play an important role in lipid transfer (7). This is based on the observation that N780Y missense mutation results in the loss of triglyceride transfer activity (7, 26). We also observed that MTP carrying this mutation has very low triglyceride transfer activity and undetectable phospholipid transfer.

Apart from apoB-containing lipoprotein assembly in mammals, MTP is required for the secretion of vitellogenin A1 in frogs (32). Vitellogenin is only secreted from COS cells when coexpressed with MTP. The secreted vitellogenin does not show flotation properties, indicative of less neutral lipid association. Interestingly, N780Y missense mutation supports secretion of vitellogenin but not of apoB (32). Because vitellogenin is secreted as a phospholipid-rich particle, we had hypothesized that N780Y might transfer phospholipids to aid in the secretion of vitellogenin. However, our studies showed that this missense mutant is also defective in phospholipid transfer activity. Therefore, MTP's chaperone activity that supports vitellogenin secretion is not related to its ability to transfer lipids. It has been shown that MTP interacts with vitellogenin (32), and this physical protein-protein interaction might be critical and sufficient for vitellogenin secretion.

In short, this study provides biochemical explanation for novel missense mutations S590I and G746E, and it expands the reasons for ABL in N780Y and R540H mutations. Apart from the absence of triglyceride transfer activity, our studies show that N780Y and R540H do not transfer phospholipids. We also found that S590I and G746E lack both triglyceride and phospholipid transfer activities. Hence, these studies point out that ABL is associated with an inability to transfer both triglycerides and phospholipids.

The authors sincerely appreciate and acknowledge Anne Lisa Cossu, who constructed the plasmids and together with I.K. generated the retroviruses. The authors also acknowledge the technical assistance of Wei Min at Downstate Confocal Core in the imaging of the immunofluorescence studies.

REFERENCES

1. Wetterau, J. R., L. P. Aggerbeck, P. M. Laplaud, and L. R. McLean. 1991. Structural properties of the microsomal triglyceride-transfer protein complex. *Biochemistry.* **30:** 4406–4412.
2. Wetterau, J. R., K. A. Combs, S. N. Spinner, and B. J. Joiner. 1990. Protein disulfide isomerase is a component of the microsomal triglyceride transfer protein complex. *J. Biol. Chem.* **265:** 9800–9807.
3. Wetterau, J. R., K. A. Combs, L. R. McLean, S. N. Spinner, and L. P. Aggerbeck. 1991. Protein disulfide isomerase appears necessary to maintain the catalytically active structure of the microsomal triglyceride transfer protein. *Biochemistry.* **30:** 9728–9735.

4. Wetterau, J. R., and D. B. Zilversmit. 1985. Purification and characterization of microsomal triglyceride and cholesteryl ester transfer protein from bovine liver microsomes. *Chem. Phys. Lipids.* **38:** 205–222.
5. Anderson, T. A., D. G. Levitt, and L. J. Banaszak. 1998. The structural basis of lipid interactions in lipovitellin, a soluble lipoprotein. *Structure.* **6:** 895–909.
6. Mann, C. J., T. A. Anderson, J. Read, S. A. Chester, G. B. Harrison, S. Köchl, P. J. Ritchie, P. Bradbury, F. S. Hussain, J. Amey, et al. 1999. The structure of vitellogenin provides a molecular model for the assembly and secretion of atherogenic lipoproteins. *J. Mol. Biol.* **285:** 391–408.
7. Read, J., T. A. Anderson, P. J. Ritchie, B. Vanloo, J. Amey, D. Levitt, M. Rosseneu, J. Scott, and C. C. Shoulders. 2000. A mechanism of membrane neutral lipid acquisition by the microsomal triglyceride transfer protein. *J. Biol. Chem.* **275:** 30372–30377.
8. Hussain, M. M., J. Shi, and P. Dreizen. 2003. Microsomal triglyceride transfer protein and its role in apolipoprotein B-lipoprotein assembly. *J. Lipid Res.* **44:** 22–32.
9. Bradbury, P., C. J. Mann, S. Köchl, T. A. Anderson, S. A. Chester, J. M. Hancock, P. J. Ritchie, J. Amey, G. B. Harrison, D. G. Levitt, et al. 1999. A common binding site on the microsomal triglyceride transfer protein for apolipoprotein B and protein disulfide isomerase. *J. Biol. Chem.* **274:** 3159–3164.
10. Bakillah, A., N. Nayak, U. Saxena, R. M. Medford, and M. M. Hussain. 2000. Decreased secretion of apoB follows inhibition of apoB-MTP binding by a novel antagonist. *Biochemistry.* **39:** 4892–4899.
11. Hussain, M. M., P. Rava, M. Walsh, M. Rana, and J. Iqbal. 2012. Multiple functions of microsomal triglyceride transfer protein. *Nutr. Metab. (Lond.).* **9:** 14.
12. Wang, S., R. S. McLeod, D. A. Gordon, and Z. Yao. 1996. The microsomal triglyceride transfer protein facilitates assembly and secretion of apolipoprotein B-containing lipoproteins and decreases cotranslational degradation of apolipoprotein B in transfected COS-7 cells. *J. Biol. Chem.* **271:** 14124–14133.
13. Atzel, A., and J. R. Wetterau. 1993. Mechanism of microsomal triglyceride transfer protein catalyzed lipid transport. *Biochemistry.* **32:** 10444–10450.
14. Atzel, A., and J. R. Wetterau. 1994. Identification of two classes of lipid molecule binding sites on the microsomal triglyceride transfer protein. *Biochemistry.* **33:** 15382–15388.
15. Rava, P., and M. M. Hussain. 2007. Acquisition of triacylglycerol transfer activity by microsomal triglyceride transfer protein during evolution. *Biochemistry.* **46:** 12263–12274.
16. Rava, P., G. K. Ojakian, G. S. Shelness, and M. M. Hussain. 2006. Phospholipid transfer activity of microsomal triacylglycerol transfer protein is sufficient for the assembly and secretion of apolipoprotein B lipoproteins. *J. Biol. Chem.* **281:** 11019–11027.
17. Khatun, I., S. Zeissig, J. Iqbal, M. Wang, D. Curiel, G. S. Shelness, R. S. Blumberg, and M. M. Hussain. 2012. Phospholipid transfer activity of MTP promotes assembly of phospholipid-rich apoB-containing lipoproteins and reduces plasma as well as hepatic lipids in mice. *Hepatology.* **55:** 1356–1368.
18. Bassen,F.A., and A. L. Kornzweig. 1950. Malformation of the erythrocytes in a case of atypical retinitis pigmentosa. *Blood.* **5:** 381–387.
19. Rader, D. J., and H. B. Brewer, Jr. 1993. Abetalipoproteinemia. New insights into lipoprotein assembly and vitamin E metabolism from a rare genetic disease. *JAMA.* **270:** 865–869.
20. Narcisi, T. M., C. C. Shoulders, S. A. Chester, J. Read, D. J. Brett, G. B. Harrison, T. T. Grantham, M. F. Fox, S. Povey, T. W. de Bruin, et al. 1995. Mutations of the microsomal triglyceride-transfer-protein gene in abetalipoproteinemia. *Am. J. Hum. Genet.* **57:** 1298–1310.
21. Sharp, D., L. Blinderman, K. A. Combs, B. Kienzle, B. Ricci, K. Wager-Smith, C. M. Gil, C. W. Turck, M-E. Bouma, D. J. Rader, et al. 1993. Cloning and gene defects in microsomal triglyceride transfer protein associated with abetalipoproteinemia. *Nature.* **365:** 65–69.
22. Shoulders, C. C., D. J. Brett, J. D. Bayliss, T. M. E. Narcisi, A. Jarmuz, T. T. Grantham, P. R. D. Leoni, S. Bhattacharya, R. J. Pease, P. M. Cullen, et al. 1993. Abetalipoproteinemia is caused by defects of the gene encoding the 97 kDa subunit of a microsomal triglyceride transfer protein. *Hum. Mol. Genet.* **2:** 2109–2116.
23. Rehberg, E. F., M. E. Samson-Bouma, B. Kienzle, L. Blinderman, H. Jamil, J. R. Wetterau, L. P. Aggerbeck, and D. A. Gordon. 1996. A novel abetalipoproteinemia genotype. Identification of a missense mutation in the 97-kDa subunit of the microsomal triglyceride transfer protein that prevents complex formation with protein disulfide isomerase. *J. Biol. Chem.* **271:** 29945–29952.
24. Yang, X. P., A. Inazu, K. Yagi, K. Kajinami, J. Koizumi, and H. Mabuchi. 1999. Abetalipoproteinemia caused by maternal isodisomy of chromosome 4q containing an intron 9 splice acceptor mutation in the microsomal triglyceride transfer protein gene. *Arterioscler. Thromb. Vasc. Biol.* **19:** 1950–1955.
25. Wang, J., and R. A. Hegele. 2000. Microsomal triglyceride transfer protein (MTP) gene mutations in Canadian subjects with abetalipoproteinemia. *Hum. Mutat.* **15:** 294–295.
26. Ohashi, K., S. Ishibashi, J. Osuga, R. Tozawa, K. Harada, N. Yahagi, F. Shionoiri, Y. Iizuka, Y. Tamura, R. Nagai, et al. 2000. Novel mutations in the microsomal triglyceride transfer protein gene causing abetalipoproteinemia. *J. Lipid Res.* **41:** 1199–1204.
27. Berthier, M. T., P. Couture, A. Houde, A. M. Paradis, A. Sammak, A. Verner, J. P. Depres, C. Gagne, D. Gaudet, and M. C. Vohl. 2004. The c.419–420insA in the MTP gene is associated with abetalipoproteinemia among French-Canadians. *Mol. Genet. Metab.* **81:** 140–143.
28. Ledmyr, H., F. Karpe, B. Lundahl, M. McKinnon, C. Skoglund-Andersson, and E. Ehrenborg. 2002. Variants of the microsomal triglyceride transfer protein gene are associated with plasma cholesterol levels and body mass index. *J. Lipid Res.* **43:** 51–58.
29. Al-Shali, K., J. Wang, F. Rosen, and R. A. Hegele. 2003. Ileal adenocarcinoma in a mild phenotype of abetalipoproteinemia. *Clin. Genet.* **63:** 135–138.
30. Di Leo, E., S. Lancellotti, J. Y. Penacchioni, A. B. Cefalu, M. Averna, L. Pisciotta, S. Bertolini, S. Calandra, C. Gabelli, and P. Tarugi. 2005. Mutations in MTP gene in abeta- and hypobeta-lipoproteinemia. *Atherosclerosis.* **180:** 311–318.
31. Ricci, B., D. Sharp, E. Orourke, B. Kienzle, L. Blinderman, D. Gordon, C. Smithmonroy, G. Robinson, R. E. Gregg, D. J. Rader, et al. 1995. A 30-amino acid truncation of the microsomal triglyceride transfer protein large subunit disrupts its interaction with protein disulfide-isomerase and causes abetalipoproteinemia. *J. Biol. Chem.* **270:** 14281–14285.
32. Sellers, J. A., L. Hou, D. R. Schoenberg, M. Batistuzzo, Sr., W. Wahli, and G. S. Shelness. 2005. Microsomal triglyceride transfer protein promotes the secretion of Xenopus laevis vitellogenin A1. *J. Biol. Chem.* **280:** 13902–13905.
33. Sellers, J. A., L. Hou, H. Athar, M. M. Hussain, and G. S. Shelness. 2003. A drosophila microsomal triglyceride transfer protein homolog promotes the assembly and secretion of human apolipoprotein B: Implications for human and insect lipid transport and metabolism. *J. Biol. Chem.* **278:** 20367–20373.
34. Bakillah, A., Z. Zhou, J. Luchoomun, and M. M. Hussain. 1997. Measurement of apolipoprotein B in various cell lines: correlation between intracellular levels and rates of secretion. *Lipids.* **32:** 1113–1118.
35. Hussain, M. M., Y. Zhao, R. K. Kancha, B. D. Blackhart, and Z. Yao. 1995. Characterization of recombinant human apoB-48-containing lipoproteins in rat hepatoma McA-RH7777 cells transfected with apoB48 cDNA: Overexpression of apoB-48 decreases synthesis of endogenous apoB-100. *Arterioscler. Thromb. Vasc. Biol.* **15:** 485–494.
36. Athar, H., J. Iqbal, X. C. Jiang, and M. M. Hussain. 2004. A simple, rapid, and sensitive fluorescence assay for microsomal triglyceride transfer protein. *J. Lipid Res.* **45:** 764–772.
37. Rava, P., H. Athar, C. Johnson, and M. M. Hussain. 2005. Transfer of cholesteryl esters and phospholipids as well as net deposition by microsomal triglyceride transfer protein. *J. Lipid Res.* **46:** 1779–1785.
38. Jones, D. T. 1999. Protein secondary structure prediction based on position-specific scoring matrices. *J. Mol. Biol.* **292:** 195–202.
39. Banaszak, L., W. Sharrock, and P. Timmins. 1991. Structure and function of a lipoprotein: lipovitellin. *Annu. Rev. Biophys. Biophys. Chem.* **20:** 221–246.
40. Anwar, K., H. J. Kayden, and M. M. Hussain. 2006. Transport of vitamin E by differentiated Caco-2 cells. *J. Lipid Res.* **47:** 1261–1273.
41. Anwar, K., J. Iqbal, and M. M. Hussain. 2007. Mechanisms involved in vitamin E transport by primary enterocytes and in vivo absorption. *J. Lipid Res.* **48:** 2028–2038.
42. Sanner, M., A. J. Olson, and J. C. Spehner. 1996. Reduced Surface: an Efficient Way to Compute Molecular Surfaces. *Biopolymers.* **38:** 305–320.